ARTICLE

Nucleation and Growth of Gold Nanoparticles Studied *via in situ* Small Angle X-ray Scattering at Millisecond Time Resolution

Jörg Polte,[†] Robert Erler,[†] Andreas F. Thünemann,[†] Sergey Sokolov,[‡] T. Torsten Ahner,[‡] Klaus Rademann,[§] Franziska Emmerling,[†,*] and Ralph Kraehnert[‡]

[†]BAM Federal Institute of Materials Research and Testing, Richard-Willstätter-Strasse 11, D-12489 Berlin, Germany, [‡]Technische Universität Berlin, Technische Chemie, Strasse des 17, Juni 124, D-10623 Berlin, Germany, and [§]Humboldt-Universität zu Berlin, Department of Chemistry, Brook-Taylor-Strasse 2, D-12489 Berlin, Germany

ABSTRACT Gold nanoparticles (AuNP) were prepared by the homogeneous mixing of continuous flows of an aqueous tetrachloroauric acid solution and a sodium borohydride solution applying a microstructured static mixer. The online characterization and screening of this fast process (~2 s) was enabled by coupling a micromixer operating in continuous-flow mode with a conventional in-house small angle X-ray scattering (SAXS) setup. This online characterization technique enables the time-resolved investigation of the growth process of the nanoparticles from an average radius of *ca.* 0.8 nm to about 2 nm. To the best of our knowledge, this is the first demonstration of a continuous-flow SAXS setup for time-resolved studies of nanoparticle formation mechanisms that does not require the use of synchrotron facilities. In combination with X-ray absorption near edge structure microscopy, scanning electron microscopy, and UV—vis spectroscopy the obtained data allow the deduction of a two-step mechanism of gold nanoparticle formation. The first step is a rapid conversion of the ionic gold precursor into metallic gold nuclei, followed by particle growth *via* coalescence of smaller entities. Consequently it could be shown that the studied synthesis serves as a model system for growth driven only by coalescence processes.

KEYWORDS: nanoparticle formation mechanism · SAXS · microstructured static mixer · continuous flow

Metallic nanoparticles have attracted much attention owing to their unique properties and numerous promising applications. In particular gold nanoparticles were investigated with regard to potential applications in biotechnology,[1] catalysis,[2] and optoelectronics.[3] In this context a profound understanding of the mechanisms and kinetics of particle formation is essential for tuning their size and morphology.

Recently we demonstrated the possibilities of combined *in situ* small-angle X-ray-scattering/X-ray near edge structure (SAXS/XANES) measurements in a solution of levitated sample droplets, where SAXS delivers information on size and shape of the formed particles. XANES can be applied to monitor the progress of the reaction by means of the oxidation state.[4] Because of experimental limitations the above-mentioned method did not reach a time resolution sufficient for one of the typical fast gold nanoparticle synthesis, that is, the reduction *via* sodium borohydride ($NaBH_4$) or ascorbic acid ($C_6H_8O_6$), which occurs in the time span of milliseconds to a few seconds. Since the acquisition time of an X-ray scattering curve is typically in the range of several minutes, such fast particle formation processes cannot be investigated by common laboratory SAXS setups using a conventional Roentgen tube. Even when using synchrotron radiation only few beamlines provide the needed time resolution in the range of 200 ms.[5] For the investigation of such rapidly proceeding liquid-phase syntheses that require a time resolution of 100—200 ms a rapid mixing of the reactant solutions is essential.

These fast syntheses can be carried out in microstructured mixers that ensure rapid local mixing. The synthesis of different materials (chalcogenides,[6,7] oxides,[8] metals[9—11]) in such mixing devices has been described in the literature. The materials produced using microstructured mixers typically show a more homogeneous constitution.[12,13]

For time-resolved SAXS analysis stopped-flow and continuous-flow techniques have been established—both including a rapid mixing device.[14—19] The stopped-flow devices usually demand synchrotron facilities for sufficiently fast data acquisition, where the achieved time resolution is limited by the characteristics of the beamline.

*Address correspondence to franziska.emmerling@bam.de

Received for review October 27, 2009 and accepted January 11, 2010.

Published online January 20, 2010. 10.1021/nn901499c

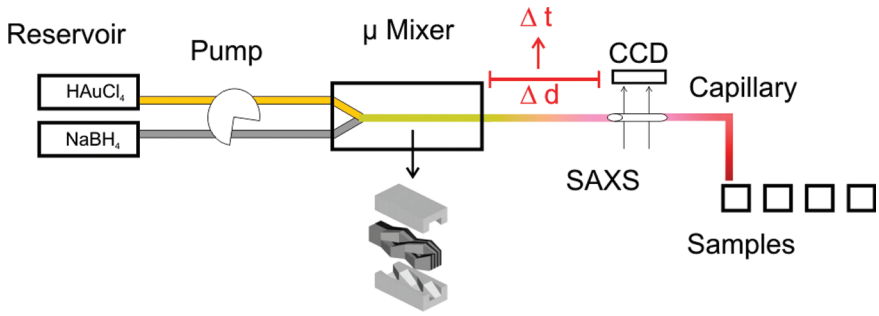

Figure 1. Experimental setup for particle synthesis in continuous-flow mode coupling a microstructured static mixer directly to SAXS-analysis in a flow cell.

In the following we present the investigation of the nucleation and growth process of gold nanoparticles *via* SAXS analysis, demonstrating that the continuous-flow technique can be applied without synchrotron radiation (see Figure 1). The setup transforms the time scale into a length scale and allows for investigating fast particle formation online without an additional sample preparation step that may alter the sample condition. To the best of our knowledge, this is the first account of coupling a microstructured synthesis reactor to a laboratory SAXS instrument for an investigation of particle formation mechanisms. The synthesis of gold nanoparticles using sodium borohydride as reducing agent was studied. On the basis of SAXS analysis a two-step mechanism of particle formation is proposed. The particles' size and shape derived from SAXS measurements in the continuous-flow setup are in good agreement with those obtained from SEM and UV−vis spectroscopy.

Full experimental details are given in the Methods section. Briefly, gold nanoparticles were synthesized by reduction of tetrachloroauric acid using sodium borohydride, both present in aqueous solution. The synthesis was carried out both in batch mode (combined with UV−vis analysis) as well as continuous flow employing a microstructured static mixer to join the solutions (combined with either SAXS or XANES analysis). The micromixer and liquid dosing was set up as illustrated in Figure 1. The interconnection of the micromixer to the SAXS instrument was established *via* a delay coil (Teflon tubing). The delay time between micromixer and SAXS instrument, that is, the variable reaction time coordinate, was adjusted varying the length and diameter of the Teflon tubing to enable SAXS analysis at different stages of the reaction. The corresponding addressable reaction times ranged from 100 ms to about 136 s. To analyze colloid samples at reaction times exceeding 140 s, liquid samples were collected at the mixer outlet and aged under stirring in a beaker. Colloid samples dried on titania-coated silicon wafers were analyzed by SEM. While SAXS data were recorded on a commercial lab-scale SAXS instrument (SAXSess, Anton Paar, Graz, Austria; equipped with X-ray generator producing Cu Kα radiation and a CCD detector), XANES spectra were recorded at excitation energies between 11889 and 11933 eV using the μ-spot beamline of BESSY II.

RESULTS AND DISCUSSION

Gold nanoparticles were synthesized in the continuous-flow setup with different residence time in the tubing downstream of the microstructured mixer. SEM images of such nanoparticles deposited as colloid on titania-coated Si-wafers are shown in Figure 2. The images show particles with diameters of < 4 nm. An increase of particle size with increasing residence time is not apparent from the images, suggesting that particle growth occurs on a much shorter time scale than suitable for SEM-sample preparation. In general, the particle size is identical to sizes obtained in batch experiments. Moreover, the size of the nanoparticles synthesized with the micromixer compares also well to data reported by Kohler *et al*. for similar experiments applying a micromixer and $NaBH_4$ as reducing agent in a continuous flow-synthesis.[20]

Improved time resolution and the option to acquire data *in situ* during the reaction is offered by UV−vis spectroscopy, which has been frequently applied to monitor the change of optical colloid properties during different AuNP synthesis procedures. The synthesis was carried out in a UV-cuvette[20] to estimate the time resolution required for following the AuNP formation using $NaBH_4$ as reducing agent.

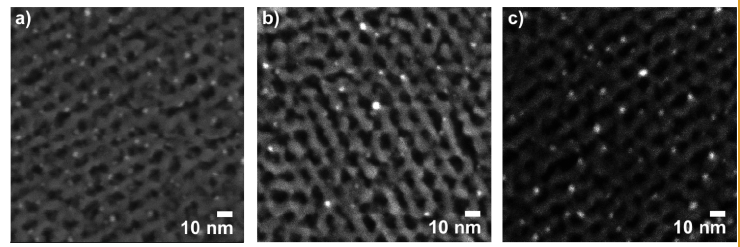

Figure 2. SEM images of the gold nanoparticles synthesized in continuous-flow mode and deposited on a substrate surface after different aging times. The images show particles deposited after *ca*. (a) 10 (b) 60 and (c) 600 s of starting the synthesis reaction by joining the reactants in the micromixer. (Bright spots correspond to gold nanoparticles, the dark spots and areas correspond to pores in the mesoporous titania employed for particle immobilization.)

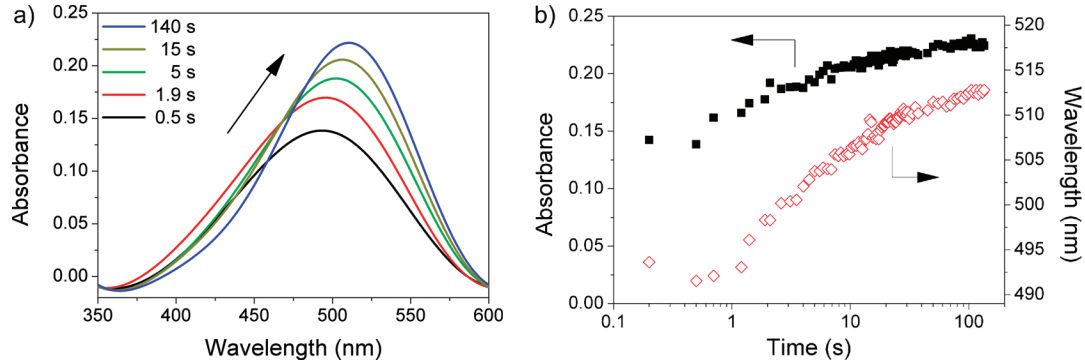

Figure 3. UV−vis data recorded *in situ* in a particle synthesis experiment carried out in batch-mode inside a UV cuvette. (a) Selected UV−vis spectra obtained during the synthesis reaction showing the evolution of the surface plasmon resonance peak (for data treatment see Methods section), (b) Intensity of absorbance and position of the plasmon resonance peak in the spectrum as a function of reaction time (log scale). An increasing absorbance and shift to higher wavelengths can be seen.

Selected UV spectra acquired at a time resolution of about 500 ms are shown in Figure 3a and correspond to the observed color change of the reaction solution turning red within *ca.* 2−3 s. The UV−vis spectra show a shift of the maximum of the absorption band from 490 nm to around 515 nm accompanied by an increase of the absorbance maximum (Figure 3a). The recorded position of the surface plasmon resonance band provides an estimate for the upper limit of the size of formed particles since the peak shifts to higher wavelengths with increasing particle size, and positions of 520−525 nm were reported for spherical gold particles of about 5−6 nm radius.[21,22]

Figure 3b shows the position and intensity of the plasmon resonance band *versus* reaction time. The rapid appearance of the band indicates a fast formation of particles, which is probably followed by a slower growth process. The data suggest that a time resolution well below 1 s is required to monitor the nucleation and growth process of AuNP synthesized *via* reduction with $NaBH_4$ at room temperature.

Contrary to uncertainties in the interpretation of UV−vis of colloidal gold particle solutions, SAXS allows a direct determination of the size, shape, and number of metal particles in solution *via* fitting of corresponding models to experimentally scattering curves. Since typical measurement times for scattering curves with conventional lab equipment are in the range of several minutes, the time resolution of *ca.* 100 ms needed to investigate the particle synthesis was established in a continuous-flow setup that coupled synthesis and SAXS analysis. Representative examples of measured scattering curves along with the corresponding fits are shown in Figure 4, confirming the quality of the obtained data. The evaluated SAXS data plotted *versus* a logarithmic time scale are shown in Figure 5, that is, radius and polydispersity (Figure 5a), number of particles (Figure 5b), particle size distribution (inset in Figure 5b), and volume fraction of gold present as particles (Figure 5c).

The rapid formation of gold particles becomes evident from Figure 5a,b, showing that already after about 100 ms numerous particles have been formed in the solution. The evaluated SAXS data indicate the formation of particles within the first 100 ms with a radius of about 0.8 nm. This particle radius is close to the resolution limit of common laboratory SAXS systems.

Subsequently, particles grow further in size up to about 1.7 nm radius (Figure 5a), accompanied by a decrease in the number of particles (Figure 5b). As evident from the logarithmic time scale in Figure 5, the growth rate of the particles decays exponentially. Polydispersity of the particles remained low, and was therefore fixed at values of 10 and 20% when evaluating scattering curves measured for colloids aged in the tube ($t <$

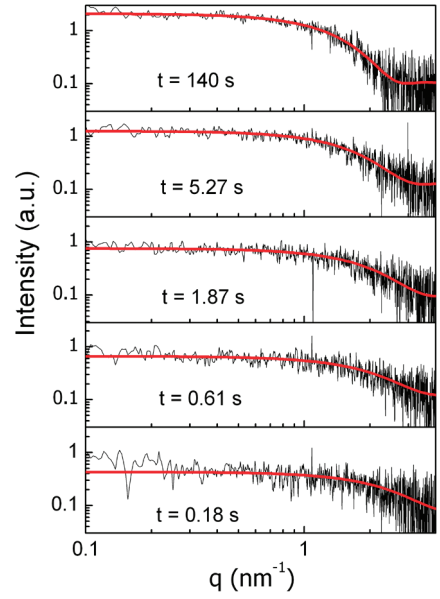

Figure 4. Representative small-angle X-ray scattering curves (black lines) recorded during the synthesis of gold nanoparticles in continuous-flow mode at different reaction times. The smooth lines indicate the respective corresponding fit by a Schultz−Zimm distribution.

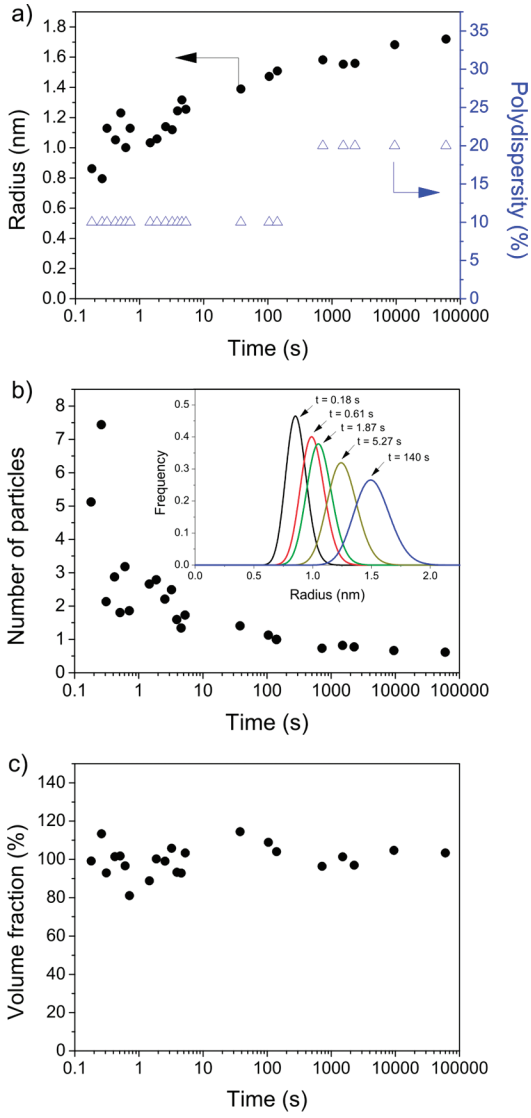

Figure 5. Evaluated SAXS data plotted *vs* reaction time (log scale) derived from scattering curves recorded during the synthesis of gold nanoparticles in continuous-flow mode. (a) Evolution of radius (bullets) and polydispersity (triangles) of gold nanoparticles throughout the reaction process. The values were derived applying a solid sphere model with a Schultz–Zimm distribution. The polydispersity was constrained to values of 10% (aging in continuous flow) and 20% (further aging in a stirred beaker). (b) The number of gold nanoparticles derived from the fit (normalized to the last measurement). Inset: Schultz–Zimm distribution of particle size at different reaction times. (c) Total volume of the gold nanoparticles calculated from the evaluated SAXS data.

136 s) or in a stirred beaker ($t > 136$ s), respectively. Assuming that the radial electron density of a gold nanoparticle is constant upon growing in radius from about 0.8 to 1.7 nm, the number of particles decreased continuously throughout the studied time interval of particle synthesis (Figure 5b). Combined with the fact that particles grow over time, the volume fraction of particles which represents the total volume of all gold nanoparticles in solution remained essentially constant throughout the experiment (Figure 5c). This observation suggests that at the first acquired experimental data point, all of the Au(III) precursor species have already been converted into Au(0) constituting the particles, and that subsequent particle growth is not related to further reduction of the Au(III) precursor compound. Direct experimental proof of such a rapid reduction leading to metallic gold was sought by XANES analysis using the same synthesis setup, that is, pump and mixer, in combination with the μ-spot beamline at the synchrotron facility BESSY II.

The XANES curves shown in Figure 6 were recorded at different stages of the particle synthesis to obtain the average oxidation state of gold species contained in the reaction solution, that is, for the Au(III) precursors prior to mixing with the reducing agent $NaBH_4$, in flow through configuration 200 ms after joining the solutions, and 20 h after joining the reactants (equal to complete conversion). A comparison of the XANES spectra reveals that the reduction process of Au(III) completes within the first 200 ms of the experiment. Confirmed by an independent analytical method the conclusion derived from SAXS analysis (Figure 5) shows that all gold is present in the form of Au(0), that is, as cluster or particle, at the latest after 200 ms of reaction time. All observed subsequent particle growth must therefore result from the coalescence of smaller nuclei into particles of growing dimensions.

The combination of presented SEM, UV–vis, SAXS, and XANES suggests that the formation of gold nanoparticles in the presence of $NaBH_4$ as strong reducing agent and in the absence of additional stabilizers occurs within two steps (see Figure 7).

The first step is the initial and rapid reduction of the gold precursor within less than 200 ms accompanied by the formation of primary particles. In a second

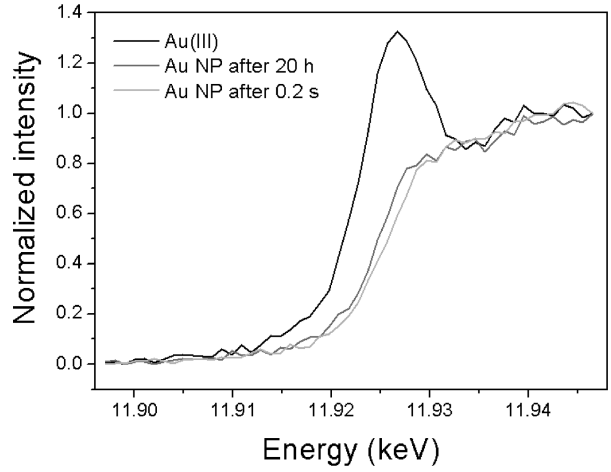

Figure 6. XANES spectra recorded in a continuous-flow experiment for a reaction time of 0.2 s after joining the reactant in the microstructured mixer (dark gray curve). As a reference the spectrum of an unreacted aqueous $HAuCl_4$ solution (black curve) is shown, indicative of the formal oxidation state Au(III), and a spectrum for a colloid after 20 h of reaction time, that is, with fully converted gold precursor, indicative of the metallic Au(0) oxidation state.

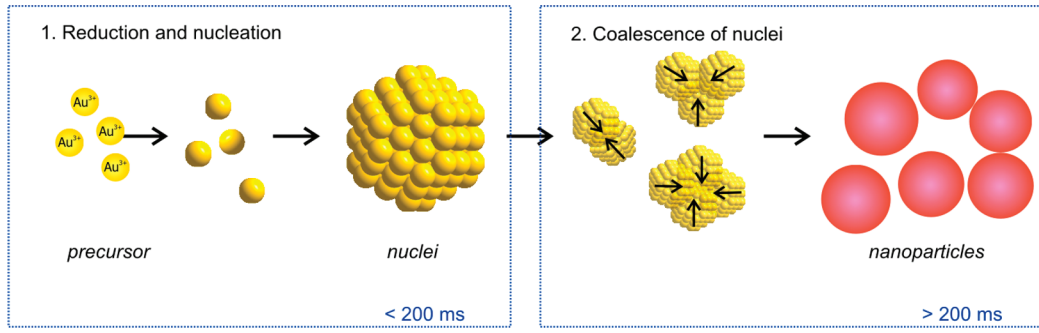

Figure 7. Schematic illustration for the deduced process of gold nanoparticle formation.

step, the primary particles grow due to coalescence along with a corresponding decrease in the number of particles. In consequence, particle growth in the studied system is in the experimentally accessible time frame driven only by coalescence, and not a mixture of monomer attachment from solution and particle coalescence.[23] Such behavior corresponds well to our recent investigations on the growth mechanisms of gold nanoparticles carried out with the same gold precursor using sodium tricitrate as reducing agent.[4] In that study, the initial formation and growth of gold particles up to 4 nm radius was also driven mainly by the coalescence of smaller primary particles, whereas the stabilizing effect of citrate became only evident for a particle radius exceeding 4 nm. Since a stabilizing agent was not present in the system, the particle growth did not come to an end even after 24 h (Figure 5a). The comparison of particle formation and growth mechanisms between the citrate and the sodium borohydride system emphasizes that particle stability and stabilization play a decisive role in determining the size and size distribution of the formed colloidal gold nanoparticles.

CONCLUSIONS

A new setup was developed that couples a microstructured mixer for fast continuous-flow mixing of reactants for nanoparticle synthesis with small-angle X-ray scattering to enable online analysis of the formed nanoparticles. The method allows "in house" SAXS at a time resolution of about 100 ms without requiring a synchrotron radiation facility. The setup is applicable in general to a wide range of chemical liquid phase syntheses of nanoparticles. It provides mechanistic and kinetic information for rapid particle formation processes in the frequently encountered case where alternative analysis methods do not offer sufficient information or time resolution.

The setup was successfully used to elucidate the process of gold nanoparticle formation employing $NaBH_4$ as reduction agent. In combination with XANES, the data show an initial rapid and complete conversion of the gold precursor into Au(0) in the form of gold nuclei, followed by particle growth exclusively *via* coalescence of the nuclei into bigger particles. That a complete conversion of the gold-precursor into metallic gold nuclei within less than 100 ms could be observed is because such rapid mixing was achieved with the applied microstructured mixer, and that the coupled SAXS analysis enabled a sufficient time resolution. The studied system constitutes a model system for nanoparticle growth driven only by coalescence of primary particles. Increasing the time resolution of the method to follow the actual nucleation process and elucidating the role of stabilizing agents remains a challenge for further studies.

METHODS

Materials. Tetrachloroauric acid ($HAuCl_4 \cdot 3H_2O$, 99.9+%) and sodium borohydride ($NaBH_4$, 99.9+%) were purchased from Aldrich. All chemicals were used as received without further purification. Ultrapure deionized water was used for the aqueous solutions.

Nanoparticle Synthesis. The synthesis of gold nanoparticles by reduction of tetrachloroauric acid using sodium borohydride was adapted from a procedure published by Wagner *et al.*[24] Briefly, 39.28 mg of tetrachloroauric acid were dissolved in 200 mL of water (Millipore) and added to 15.10 mg of sodium borohydride dissolved in 200 mL of water. Solutions of $NaBH_4$, were prepared freshly for each experiment.

Microstructured Mixer. A microstructured static caterpillar mixer CPMM R600 SO (IMM, Mainz, Germany) was used at a total liquid flow rate of 50 mL min^{-1} to continuously join and mix equal volumes of the two respective reactant solutions according to the split-and-recombine mixing principle. The mixing device is described elsewhere.[25]

SAXS Instrument. Small angle X-ray scattering is a common method to determine the shape and size of particles in colloidal solution. The measured scattering signal originates from the contrast between the growing nanoparticles and the solvent. The scattering vector q is defined in terms of the scattering angle 2θ and the wavelength λ of the radiation: thus $q = 4\pi/\lambda \sin(\theta/2)$. A detailed overview on SAXS data evaluation procedure using model fit functions is given by Pedersen.[26]

The applied SAXS instrument (SAXSess, Anton Paar, Graz, Austria) is a modern version of the classical "Kratky camera" which is described in detail elsewhere.[27] Focusing multilayer optics and a slit collimation provide an intense monochromatic primary beam with low background. The system was attached to a conventional X-ray generator (PANalytical, Kassel, Germany) equipped with a sealed X-ray tube (Cu anode target type, producing Cu Kα X-rays with a wavelength $\lambda = 0.154$ nm) operating at 40 kV and 50 mA. The scattered X-ray intensities were measured with a CCD detection system (Roper Scientific, Ottobrunn,

Germany) and processed with SAXSQuant software (version 2.0). Scattering curves were acquired in sequences of 20 individual curves of 10 s each and averaged prior to further processing. The curve fitting was carried out using SANS Analysis 3_v3.00[28] implemented in the software suite IGOR.[29]

Evaluation of SAXS Data. The derived experimental scattering curves were fitted with a model which describes the scattered intensity of hard spheres having a Schultz−Zimm size distribution. The Schultz−Zimm distribution is given by

$$f(r) = (z+1)^{z+1}x^{z}\frac{\exp[-(z+1)x]}{R_{Avg}\Gamma(z+1)} \quad (1)$$

where R_{Avg} is the mean radius, $x = r/R_{Avg}$, z is related to the polydispersity ($p = \sigma/R_{Avg}$) by $z = 1/p^2 - 1$, where σ^2 is the variance of the distribution.

In a diluted system the scattering intensity of the particles can be assumed to be proportional to the form factor of a single particle. The scattering intensity of monodisperse hard spheres with volume V is given by

$$I(q,r) = \text{scale}\cdot P(qr) = \text{scale}\cdot\left[\frac{3V(\Delta\rho)(\sin(qr) - qr\cos(qr))}{(qr)^3}\right]^2 \quad (2)$$

where $P(qr)$ is the form factor of a single hard sphere and $\Delta\rho$ the scattering length density.

In the case of polydisperse spherical particles, the sum of the scattering intensities over all particle sizes has to be taken in account, weighted by their frequency or to integrate using a size distribution function, respectively. It is common to apply the Schulz−Zimm distribution for polydisperse particles.[30] Hence the scattering intensity is given by

$$I(q) = \text{scale}\cdot\int_0^\infty f(r)\,P(qr)\,dr \quad (3)$$

An analytical solution of that integral can be found in Kotlarchyk *et al.*[31]

To analyze the nucleation and growth mechanism of nanoparticles the number of particles is important. This information can be obtained by using the general relation of $I(q = 0)$ for a single particle, which is independent of its shape and size, that is, $I_S = (\Delta\rho)^2V^2$. Thus the scattered intensity $I(q = 0)$ of polydisperse particles can be written as

$$I(q=0) = N\langle V^2\rangle(\Delta\rho)^2 \quad (4)$$

where N is the number of particles and $\langle V^2\rangle$ the mean value of V^2. Because of the overlapping of the scattering intensity with the primary beam $I(q = 0)$ cannot be measured directly, but is accessible *via* the extrapolation of $I(q)$ for $q \to 0$.

Experimental Setup. The micromixer and liquid dosing was set up as illustrated in Figure 1. The interconnection of the micromixer to the SAXS instrument was established *via* a delay coil (Teflon tubing). The solutions were transported *via* peristaltic pump (Ismatec Laboratoriumstechnik GmbH, Wertheim-Mondfeld, Germany) at a flow rate of 50 mL min^{-1} through a flow capillary (quartz, inner diameter of 1 mm and wall thickness of 10 μm, Anton Paar, Graz, Austria) embedded in the SAXS instrument. The delay time between micromixer and SAXS instrument, that is, the variable reaction time coordinate, was adjusted varying the length and diameter of the Teflon tubing between the two devices to enable the SAXS analysis at different stages of the reaction. The corresponding addressable reaction times ranged from 100 ms (19 cm tube length at 1 mm diameter) to about 136 s (10 m tube length at 3.8 mm diameter). To analyze colloid samples at reaction times exceeding 140 s, liquid samples were collected at the mixer outlet and aged under stirring in a beaker. SAXS data on such samples were recorded injecting the aged batch solution directly into the flow cell.

Tubing, flow capillary, and glassware were cleaned with aqua regia, water, and isopropyl alcohol prior to each experimental run. Successful cleaning of the SAXS capillary was confirmed by recording a scattering curve of ultrapure deionized water.

UV−Visible Spectroscopy. UV absorbance spectra were recorded on an AvaSpec-2048TEC-2 equipped with a Deuterium halogen light source (Avantes, Broomfield, USA), connected to a 10 mm optical path length cuvette holder *via* fiber optical cables. The UV spectra were corrected for background and the maxima were fitted applying a Gaussian curve fit. The UV spectra were smoothed using a FFT lowpass filter. Spectra were recorded *in situ* during the AuNP synthesis adding equal volumes of both reactant solutions at room temperature under mechanical stirring to the cuvette, followed by repeated spectra acquisition at 500 ms time intervals.

Scanning Electron Microscopy (SEM). The imaging of nanoparticle samples was performed on a JEOL JSM-7401F (Hitachi Ltd., Tokyo, Japan) with an acceleration voltage of 10 kV at working distance of 7 mm. To minimize effects of particle aggregation and growth during sample preparation, such as evaporation of the solvent, solutions were spin-coated on the silicon substrate. The latter was coated with a mesoporous nanocrystalline titania thin-film to ensure enhanced surface conductivity, thus reducing surface charging and improving a higher spatial resolution of the microscopic images.

X-ray Absorption near Edge Spectroscopy (XANES). XANES measurements were performed at the μSpot beamline of BESSY II.[32] The beam was monochromatized using the double-crystal monochromator (DCM) installed at the beamline. Harmonics were suppressed and the beam was focused by a curved mirror. This constellation enables a precise energy adjustment with an energy resolution of about 0.00015, that is, 1.8 eV at the energy of the Au LIII edge (11.919 keV). The excitation energy was varied from 11889 to 11933 eV in steps of 1.2 eV, resulting in 20 recorded XANES-channels. The fluorescence radiation of the sample was detected at an angle of approximately 90° with respect to the X-ray beam. The intensity of the emitted fluorescence radiation is proportional to the absorption, thus the obtained excitation spectra are equivalent to conventional absorption spectra. The X-ray fluorescence of the Au Lα line was detected with a silicon drift detector (SDD). XANES was applied to a gold foil and to a $HAuCl_4$ solution as reference. All measured XANES spectra were normalized to 0 at the lowest and 1 at the highest used excitation energy.

Acknowledgment. R.K. gratefully acknowledges generous funding by BMBF within the frame of the Nanofutur program (FKZ 03 × 5517).

REFERENCES AND NOTES

1. Storhoff, J. J.; Elghanian, R.; Mucic, R. C.; Mirkin, C. A.; Letsinger, R. L. One-Pot Colorimetric Differentiation of Polynucleotides with Single Base Imperfections Using Gold Nanoparticle Probes. *J. Am. Chem. Soc.* **1998**, *120*, 1959–1964.
2. Bond, G. C.; Louis, C.; Thompson, D. T. *Catalysis by Gold*; Imperial College Press: London, 2006; Vol. 6.
3. Treguer, M.; Rocco, F.; Lelong, G.; Le Nestour, A.; Cardinal, T.; Maali, A.; Lounis, B. Fluorescent Silver Oligomeric Clusters and Colloidal Particles. *Solid State Sci.* **2005**, *7*, 812–818.
4. Polte, J.; Ahner, T.; Delissen, F.; Sokolov, S.; Emmerling, F.; Thunemann, A. F.; Kraehnert, R. Mechanism of Gold Nanoparticle Formation in the Classical Citrate Synthesis Method Derived from Coupled *in Situ* XANES and SAXS Evaluation. J. Am. Chem. Soc., published online January 7, 2010, http://dx.doi.org/10.1021/ja906506j.
5. Narayanan, T.; Diat, O.; Bosecke, P. SAXS and USAXS on the High Brilliance Beamline at the ESRF. *Nucl. Instrum. Meth. A* **2001**, *467*, 1005–1009.
6. Yen, B. K. H.; Gunther, A.; Schmidt, M. A.; Jensen, K. F.; Bawendi, M. G. Microfabricated Gas−Liquid Segmented Flow Reactor for High-Temperature Synthesis: The Case of CdSe Quantum Dots. *Angew. Chem., Int. Ed.* **2005**, *44*, 5447–5451.
7. Chan, E. M.; Alivisatos, A. P.; Mathies, R. A. High-Temperature Microfluidic Synthesis of CdSe Nanocrystals

in Nanoliter Droplets. *J. Am. Chem. Soc.* **2005**, *127*, 13854–13861.
8. Abou Hassan, A.; Sandre, O.; Cabuil, V.; Tabeling, P. Synthesis of Iron Oxide Nanoparticles in a Microfluidic Device: Preliminary Results in a Coaxial Flow Millichannel. *Chem. Commun.* **2008**, 1783–1785.
9. Kohler, J. M.; Held, M.; Hubner, U.; Wagner, J. Formation of Au/Ag Nanoparticles in a Two Step Micro Flow-through Process. *Chem. Eng. Technol.* **2007**, *30*, 347–354.
10. Wagner, J.; Kohler, J. M. Continuous Synthesis of Gold Nanoparticles in a Microreactor. *Nano Lett* **2005**, *5*, 685–691.
11. Weng, C. H.; Huang, C. C.; Yeh, C. S.; Lei, H. Y.; Lee, G. B. Synthesis of Hexagonal Gold Nanoparticles Using a Microfluidic Reaction System. *J. Micromech. Microeng.* **2008**, *18*, 1–8.
12. Guillemet-Fritsch, S.; Aoun-Habbache, M.; Sarrias, J.; Rousset, A.; Jongen, N.; Donnet, M.; Bowen, P.; Lemaitre, J. High-Quality Nickel Manganese Oxalate Powders Synthesized in a New Segmented Flow Tubular Reactor. *Solid State Ionics* **2004**, *171*, 135–140.
13. Tsunoyama, H.; Ichikuni, N.; Tsukuda, T. Microfluidic Synthesis and Catalytic Application of PVP-Stabilized, Similar to 1 nm Gold Clusters. *Langmuir* **2008**, *24*, 11327–11330.
14. Bolze, J.; Peng, B.; Dingenouts, N.; Panine, P.; Narayanan, T.; Ballauff, M. Formation and Growth of Amorphous Colloidal $CaCO_3$ Precursor Particles as Detected by Time-Resolved SAXS. *Langmuir* **2002**, *18*, 8364–8369.
15. Pontoni, D.; Narayanan, T.; Rennie, A. R. Pontoni Time-Resolved SAXS Study of Nucleation and Growth of Silica Colloids. *Langmuir* **2002**, *18*, 56–59.
16. Abecassis, B.; Testard, F.; Spalla, O.; Barboux, P. Probing *in Situ* the Nucleation and Growth of Gold Nanoparticles by Small-Angle X-ray Scattering. *Nano Lett.* **2007**, *7*, 1723–1727.
17. Schmolzer, S.; Grabner, D.; Gradzielski, M.; Narayanan, T. Millisecond-Range Time-Resolved Small-Angle X-ray Scattering Studies of Micellar Transformations. *Phys. Rev. Lett.* **2002**, *88*, 258301.
18. Lamb, J. S.; Zoltowski, B. D.; Pabit, S. A.; Crane, B. R.; Pollack, L. Time-Resolved Dimerization of a Pas-Lov Protein Measured with Photocoupled Small Angle X-ray Scattering. *J. Am. Chem. Soc.* **2008**, *130*, 12226–12227.
19. Wu, Y.; Kondrashkina, E.; Kayatekin, C.; Matthews, C. R.; Bilsel, O. Microsecond Acquisition of Heterogeneous Structure in the Folding of a Tim Barrel Protein. *Proc. Natl. Acad. Sci. U.S.A.* **2008**, *105*, 13367–13372.
20. Haiss, B.; Thanh, N. T. K.; Aveyard, J.; Fernig, D. G. Determination of Size and Concentration of Gold Nanoparticles from UV-vis Spectra. *Anal. Chem.* **2007**, *79*, 4215–4221.
21. Pong, B. K.; Elim, H. I.; Chong, J. X.; Ji, W.; Trout, B. L.; Lee, J. Y. New Insights on the Nanoparticle Growth Mechanism in the Citrate Reduction of Gold(III) Salt: Formation of the Au Nanowire Intermediate and Its Nonlinear Optical Properties. *J. Phys. Chem. C* **2007**, *111*, 6281–6287.
22. Hussain, I.; Graham, S.; Wang, Z. X.; Tan, B.; Sherrington, D. C.; Rannard, S. P.; Cooper, A. O.; Brust, M. Size-Controlled Synthesis of Near-Monodisperse Gold Nanoparticles in the 1−4 nm Range Using Polymeric Stabilizers. *J. Am. Chem. Soc.* **2005**, *127*, 16398–16399.
23. Zheng, H. M.; Smith, R. K.; Jun, Y. W.; Kisielowski, C.; Dahmen, U.; Alivisatos, A. P. Observation of Single Colloidal Platinum Nanocrystal Growth Trajectories. *Science* **2009**, *324*, 1309–1312.
24. Wagner, J.; Tshikhudo, T. R.; Koehler, J. M. Microfluidic Generation of Metal Nanoparticles by Borohydride Reduction. *Chem. Eng. J.* **2008**, *135*, S104–S109.
25. Löb, P.; Löwe, H.; Hessel, V. Fluorinations, Chlorinations and Brominations of Organic Compounds in Micro Reactors. *J. Fluor. Chem.* **2004**, *125*, 1677–1694.
26. Pedersen, J. S. Analysis of Small-Angle Scattering Data from Colloids and Polymer Solutions: Modeling and Least-Squares Fitting. *Adv. Colloid Interface Sci.* **1997**, *70*, 171–210.
27. Bergmann, A.; Orthaber, D.; Scherf, G.; Glatter, O. Improvement of SAXS Measurements on Kratky Slit Systems by Gobel Mirrors and Imaging-Plate Detectors. *J. Appl. Crystallogr.* **2000**, *33*, 869–875.
28. *NIST*, 3.00 ed.; National Institute for Standards and Technology (NIST): Gaithersburgh, MD, 2006.
29. I.P. 6. In *IGOR Pro 6*, 6.0.0.0 ed.; WaveMetrics, Inc., Lake Oswego, OR, 2007.
30. Kotlarchyk, M.; Stephens, R. B.; Huang, J. S. Study of Schultz Distribution to Model Polydispersity of Microemulsion Droplets. *J. Phys. Chem.* **1988**, *92*, 1533–1538.
31. Kotlarchyk, M.; Chen, S. H. Analysis of Small-Angle Neutron-Scattering Spectra from Polydisperse Interacting Colloids. *J. Phys. Chem.* **1983**, *79*, 2461–2469.
32. Paris, O.; Li, C. H.; Siegel, S; Weseloh, G.; Emmerling, F.; Riesemeier, H.; Erko, A.; Fratzl, P. A. New Experimental Station for Simultaneous X-ray Microbeam Scanning for Small- and Wide-Angle Scattering and Fluorescence at Bessy II. *J. Appl. Crystallogr.* **2007**, *40*, S466–S470.